Existence of Conformers Revealed by Spectral Analysis of Single Molecules of Perylene Orange in Thin Sol−Gel Films

Carine Julien, Anne Débarre,* Daniele Nutarelli, Alain Richard, and Paul Tchénio

Laboratoire Aimé Cotton, UPR 3321 CNRS, Bâtiment 505, 91405 Orsay Cedex, France

Received: September 30, 2005; In Final Form: December 29, 2005

This paper reports on the spectral dynamics of perylene orange in thin sol−gel films. The studies are performed at the single molecule level to retrieve local information on such samples. The fluorescence spectrum of a molecule depends on the properties of the molecule itself and especially on its conformation in the ground state and in the state reached after excitation. Studies have been performed at room temperature and at a lower temperature, around 173 K. A large number of the recorded spectra reflect dual fluorescence. It is the rule at room temperature. However, at low temperature, single molecules either are relatively free to change conformation or are caught in a rigid environment. In the latter case, they present the spectrum of a rigid dye and we have identified the signature of several conformers of perylene orange in the ground state.

I. Introduction

Perylene derivatives have attracted much interest for a long time, as dyestuffs and solar concentrators. Much effort was devoted in the late 1980s to the synthesis and study of the luminescence properties of this family of molecules,[1−3] and then to their lasing properties.[4,5] The first efficient lasing effect was observed for bis((2,6-dimethylphenyl)imide) substituted perylene (DXP) by Sadraï and Bird.[6] More recently, attention was focused on the opportunity to exploit their conductive and optical properties when doped into solid matrixes, especially into sol−gels. One aim was to develop cheap and versatile solid-state lasers. Indeed, efficient or long-lasting laser effects have been reported for particular perylene derivatives, for example, DXP, perylene orange, and perylene red.[7−10] The photophysical properties of dyes dispersed in sol−gels can be rather different from those in liquids or in polymers. If the photostability of perylene orange is generally enhanced in sol−gels, a reduced quantum efficiency has also been reported in sol−gels prepared by hydrolysis of tetramethyl orthosilicate (TMOS) compared, for instance, to its value in an ethyl acetate solution.[11] The mechanisms that govern fluorescence characteristics depend both on the intrinsic properties of the molecule itself and on the particular properties of the sol−gel. In fact, the sol−gel route is a versatile way to process solid samples with variable porosity, polarity, and rigidity, properties that can be partly controlled by the choice of the precursors, solvents, and synthesis protocol. These properties are also subject to vary with respect to the sol−gel form, monolith or film. Single molecule spectroscopy (SMS) is a suitable tool to derive information on these properties at the nanoscale, by monitoring the fluorescence of doping molecules acting as nanoreporters. SMS thus opens the way to an efficient cartography of the photochemical parameters of the sample. Indeed, detailed knowledge of specific sol−gel matrixes has been derived in this way, especially by Higgins et al.[12,13]

The present work has two aims. First, it is devoted to gaining insight into the properties of thin ormosil-type sol−gel films with perylene orange acting as a probe. In fact, the intrinsic properties of sol−gel films such as their porosity and structural characteristics are far less known that those of the thickest, much studied sol−gel samples. Second, the study intends to derive a better understanding of the properties of the perylene orange molecule itself, which has proved to be a good candidate for a long-lasting laser effect. The rapid bleaching of the fluorescent probe is one of the main difficulties of SMS. In particular, the use of some of the powerful tools offered by SMS, such as spectral analysis, requires a long surviving fluorescence. Here, the choice of perylene orange as the nanosensor, in addition to the above-mentioned intrinsic interest it presents, relies on its known photostability in sol−gel monoliths.[7,9] We have performed a first study of photobleaching in our thin samples that confirmed the quite long survival time of the emitters in sol−gel films,[14,15] in agreement with the long-lasting laser effects of perylene orange observed in sol−gel monoliths.

This study has also revealed that the fluorescence efficiency was not very strong, in line with the reduced efficiency already observed in sol−gel monoliths prepared with tetramethyl orthosilicate.[11] In addition, the photochemical properties of perylene orange in these films could not be completely described by a classical five electronic level system, which led us to propose that a long-lived state should be involved in the excitation−deexcitation cycle of the dye entrapped in the sol−gel. To refine our understanding of this process, we have performed a spectral analysis of single molecule fluorescence. This study has been conducted under vacuum, both at ambient temperature and at a temperature of about 173 K. The comparison between the different behaviors observed in the two situations has allowed us to clarify some specific properties of perylene orange in sol−gel films. After a brief recall of the experimental details, the following part of the paper is devoted to discussing some particular characteristics of the spectral signatures of single molecules at low temperature and at room temperature. The recurrent observation of spectra with typical features has permitted us to define several classes of spectra. We discuss possible interpretations of these different classes and their temporal dynamics when available, in relation to both the specificities of the doping molecule and those of the sol−gel samples.

* Corresponding author. E-mail: anne.debarre@lac.u-psud.fr.

10.1021/jp055583j CCC: $33.50
Published on Web 02/04/2006

II. Experimental Section

II.1. Sol−Gel Sample. Methyltriethoxysilane ($(CH_3)Si(OC_2H_5)_3$, MTEOS) has been used as the precursor to elaborate the studied sol−gel samples of ormosil type. On average, this type of sol−gel is less polar than sol−gels obtained by using tetraalkoxysilane as a precursor, and favors a better dispersion of the perylene orange molecules in the sample. The acid hydrolysis of MTEOS is performed in an equimolar ethanol−water solution mixture. Hydrolysis solvents are then removed and replaced by a weakly doped perylene orange−THF (tetrahydrofuran) solution. The final concentration of dopants in the sol is 10^{-11} M. The sol is allowed to age in the dark, and then it is spin-coated on clean coverslips at 8000 rpm to reach film thicknesses varying between 50 and 100 nm. The mean distance between adjacent molecules in the final sol−gel film is on the order of a few micrometers.

II.2. Spectroscopic Measurements. The experimental setup is built around a wide-field microscope which allows us to acquire fluorescence images of a whole region of the studied sample. The excitation light is provided by an argon ion laser at 514 nm. The beam is coupled into the entry of a single-mode fiber, which acts as a point source. A telescope composed of two achromatic lenses images the fiber face onto the back focal plane of the objective. Between the two lenses, an adjustable pinhole placed in the plane conjugated with the sample plane acts as a field aperture and helps us obtain an illumination as uniform as possible. A narrow-band excitation filter is added in the incoming path before reflection into the objective. The typical illuminated area of the sample is then on the order of 2000 μm^2 when a 40× NA1.3 oil immersion objective is used. The Airy spot diameter is 480 nm. It determines the size of the fluorescence spot of the molecules in the image. The fluorescence of the molecules is backward collected by the same objective and sent to a CCD camera (CoolSnap HP, Roper Scientific) through the $f = 160$ mm tube lens. An Alpha Epsilon edge filter (Omega AELP 520) eliminates the residual laser light in the detection path. The total detection efficiency is estimated to be 10%. Contrary to confocal microscopy, wide-field illumination does not involve spatial filtering in the image plane. The background signal is greatly eliminated in our case because of the thinness and transparency of the sol−gel films. The sample is held in a chamber connected to a fluidic system, which allows us to work under inert atmosphere or under a vacuum of about 10^{-4} mbar. A commercial chamber is used to cool the sample down to liquid nitrogen temperature (Linkam Scientific Instruments Ltd.). Studies reported in the present paper have been performed either at room temperature around 293 K or at low temperature near 173 K and under vacuum in both cases. At the concentration of 10^{-11} M in the sol before spin casting, about 200 emitters fluoresce in the illuminated area of 2000 μm^2. As mentioned in our previous study of photobleaching on the same samples,[15] we have systematically made polarization controls at different steps of the imaging process to be sure that every analyzed bright spot corresponds to a single molecule and not to a small cluster or to an impurity. A thin Wollaston prism has been inserted into the detection path, allowing us to compare the relative intensities of two-orthogonal polarizations of the fluorescence emission under a linearly polarized excitation. For most of the bright objects, the two components are not equal, which indicates that the emission is polarized and eliminates the possibility that it could be a cluster. In a few other cases, the two components are nearly equal. It can be either a cluster of molecules, despite the low concentration of dopants, a single molecule with a dipole perpendicular to the sample or at 45° to the excitation polarization, or even a single molecule rapidly tumbling in a pore. These rare objects have been removed from the present spectral analysis. Moreover, we have recorded the temporal trace of the fluorescence of a very large number of bright objects in our samples. Their analysis reveals that we are in the single molecule regime. In contrast to the present report, many classical studies on the ability of sol−gels to be efficient solid dye laser have used high dye concentration in the range 10^{-3}−10^{-5} M, and aggregation has been frequently questioned.[10] In our case, the discussed spectra and relevant dynamics are those of single molecules, excluding dimers or larger clusters.

To gain additional information beyond fluorescence imaging, we have added a channel of spectral analysis on the side port of the microscope. Depending on the optics, up to 80% of the fluorescence can be directed to this lateral port and the 20% left is used for wide-field imaging (bottom port). Two methods have been used to record the fluorescence spectra of the molecules excited in the wide field and observed on the fluorescence images. The first one is a classical confocal detection of the fluorescence of given molecules. In the second method, the image plane of the side port is directly imaged on the entrance slit of the spectrometer, which acts as a spatial filter. The latter method has the advantage of a most efficient collection on one hand and of a possible parallel analysis of several molecules on the other hand. An additional light source can be switched on to image backward the slit onto the main image plane of the microscope, which permits us to select the rectangular area of the image that will be analyzed. In both methods, single fluorescence images are continuously acquired. This allows us to choose the molecules for spectral analysis and to check their dynamics of blinking or photobleaching. The spectral resolution is on the order of 4 cm^{-1}. The acquisition time ranges from 2 to 30 s, depending on the fluorescence efficiency of the molecules. Most often a good compromise for signal-to-noise ratio is obtained for an acquisition time of 10 s. We have also acquired successive spectra to follow the spectral dynamics of the emission, when possible. The lag time between two successive spectra corresponds to the CCD readout time, and is negligible.

III. Results and Discussion

III.1. Evidence for Conformers in the Ground State. Generally speaking, the numerous fluorescence spectra recorded display a somewhat large variety of characteristics. They differ not only in the number and widths of their lines, if they are structured, but also by the absolute energy position of the peaks and by their spacing. We have indeed observed classical fluorescence spectra, featuring a main line and the classical related vibrational structure on the red-wavelength side, more or less obscured depending on the width of the spectrum as displayed in Figure 1A. The vibrational progression of the 0−0′ and 0−1′ transitions of perylene orange has been determined in macroscopic measurements for perylene in solution in ethyl acetate,[11] in chloroform,[5] and in sol−gel monoliths,[9] and the spacing is on the order of 30−50 nm. Here, contrary to the spectra of fluorescence recorded by Higgins et al. on single molecules of Nile Red in sol−gel films,[16] more than half of the spectra we have observed (about 60% of the total) depart from such a classical fluorescence structure, as illustrated by one type of characteristic spectra in Figure 1B.

We have recorded several types of spectra at low temperature. The spectral heterogeneity partly reflects the known heterogeneity of the sol−gel sample. Nevertheless, the existence of

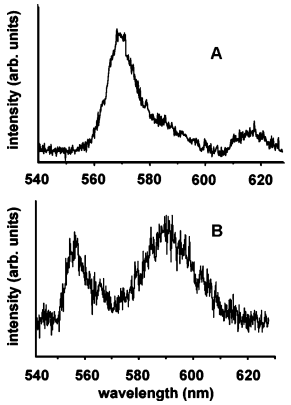

Figure 1. Two different types of spectra, recorded at different locations in a sol−gel film for two single molecules, at low temperature: (A) normal fluorescence spectrum; (B) abnormal dual fluorescence (see Figure 5C). Acquisition time 10 s; excitation wavelength 514 nm.

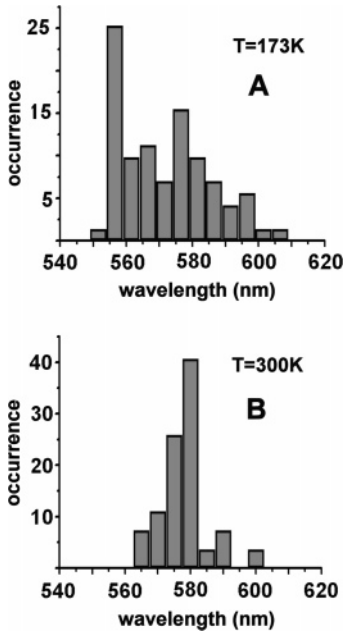

Figure 2. Distribution of fluorescence maxima: (A) low temperature; (B) room temperature. Same recording conditions as in Figure 1.

different classes of spectra, rather than a continuous variation, suggests that the chemical nature and the related structure of perylene orange itself play a role in the occurrence of the different types of spectra. Figure 2 displays the wavelength histograms at room temperature (RT) and at low temperature (LT) of the most intense fluorescence line. A striking point is that the dispersion of the maxima at room temperature is much reduced from that at 173 K. Furthermore, in the latter case a clear maximum in the distribution occurs around 557 nm, which is not observed at room temperature. To gain some insight into these results, we have grouped spectra into different classes and tentatively tried to correlate them to specific characteristics of the studied samples.

Let us first focus on a first type of spectrum that has only been observed at LT, the so-called type I spectrum in the following. It is composed of a single line that is structured on the high-wavelength side. It represents about 20% of the spectra departing from classical fluorescence spectra. The thinner the line, the more pronounced is the structure. This structure presents one bump, corresponding to a line much weaker than the main line, as depicted in Figure 3. The spacing of 10 nm between the main line and the bump is nearly constant from one spectrum

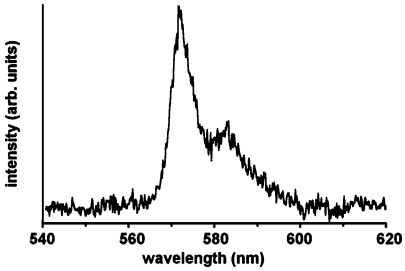

Figure 3. Representative type I single molecule fluorescence spectrum at low temperature. See text. Same experimental conditions as in Figure 1.

to another. This value is too small to correspond to the vibrational progression of the $0-0'$ and $0-1'$ transitions of perylene orange. Furthermore, the wavelength position of the main line is not constant but takes discrete values such as 565, 574, and 585 nm and rarely 609 nm. Despite the limited number of molecules displaying this kind of spectra, the observed trend is that the dispersion around these values is far smaller than the spacing between two consecutive peak wavelength values. The discrete values of peak positions measured for such spectra preclude that the distribution could result from the variable polarity of the sites inside the matrix, which would instead lead to a continuous distribution of the main line wavelength. The additional line, 10 nm from the central one, could result from an efficient coupling of the electronic transition with the $\approx$300 cm^{-1} out-of-plane C−C−C bend mode of the perylene core. In their work on perylene derivatives substituted in the bay position, Hofkens et al. have demonstrated that a twist of the two moieties of the perylene core results in a blurring and a broadening of the vibrational progression.[17] The observation in type I LT spectra of vanishingly weak vibrational bands apart from the bump suggests in turn that the perylene core is not flat at such locations.

The characteristics of type I spectra are signatures of constraints applied on the relevant molecules. Two factors at least can contribute to reduce the vibrational motions of the molecule. First, the molecule can be entrapped in a small site of high rigidity where the perylene diimide core could acquire a slight curvature, eventually including a twist of the perylene moieties. As a matter of fact, rigidity can lead both to a complete inhibition of the reconformation of the molecule and to very slow changes. At room temperature, the dynamics is increased, which could partly explain why we do not observe similar type I spectra. Conformational jumps can be fast with respect to the acquisition time and result in the observation of spectra with a single broad line of weak intensity. The second factor to be considered in terms of constraints is the fact that the site can be filled or partly filled with residual solvent. The increase of viscosity at low temperature would hinder molecular motions. As a result, in such a site, limited relaxation should occur after excitation of the molecule to the Franck−Condon state and the fluorescence spectrum could present a single line, possibly structured. If water, for example, is entrapped in close pores, freezing would inhibit intramolecular relaxation.

To proceed further in the interpretation, let us turn to the structure of perylene orange. It is a perylene diimide, with two substituted pendant phenyl groups (Chart 1). The substituents in the 2,6-positions of the phenyl groups have been chosen bulky enough to have a large steric hindrance effect maintaining the ortho position of the phenyl groups in the ground state.[3] This explains the rather high solubility of this dye. Unfortunately, no detailed crystallographic study of perylene orange itself is available, but it has been performed on some closely related

CHART 1: Structure of Perylene Orange

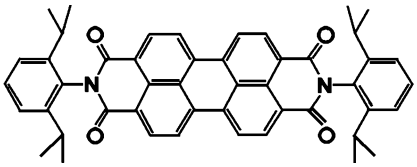

perylene-3,4,9,10-bis(dicarboximide) pigments, and especially on DXP, which differs from perylene orange only by the CH_3 substituents of the phenyls.[18,19] The results demonstrate that, in the latter molecule, the substituted phenyl rings form angles of 80.6° and 82.9°, respectively, with the flat perylene tetracarboxylic diimide moiety. Furthermore, the ground-state energy for torsion of the phenyl groups is predicted to be flat around the three minima corresponding to different twisted ground-state conformers.[6] Their energy barrier is on the order of the thermal energy at room temperature. It is thus reasonable to interpret type I spectra as the signature of the existence of several conformers varying by their ground-state twist angle. The LT results indicate that the energy barrier between them is higher than the relevant LT thermal energy of about 120 cm^{-1}. By contrast, at room temperature, the relevant spectra are broad and often very weak. This can mean that the energy barrier between the configurations is on the order of the RT thermal energy of ≈200 cm^{-1}, which favors fluctuations of the ground-state conformation on the scale of the acquisition time. The broadening of type I spectra at room temperature can also be linked to vibrational motions, which even in a small pore would be less constrained than at low temperature, thus increasing the probability for the molecule to undergo conformation changes.

III.2. Comparison between Low- and Room-Temperature Spectra. Let us focus more closely on the wavelength histograms of the maxima of the fluorescence spectra acquired at low temperature and at room temperature (Figure 2). At low temperature, the histogram shows a peak in the distribution at a wavelength of 557 nm, followed by a broad distribution including a less pronounced secondary maximum around 585 nm. At room temperature, under vacuum, the histogram shows a less broad distribution. One marked difference is the absence of a blue wing contribution at room temperature. A typical RT spectrum is displayed in Figure 4. The spectrum is dominated by a structureless broad line around 580 nm (LW line, long-wavelength line). It generally includes a weaker line at shorter wavelength around 540 nm (SW line) (and sometimes another one around 555 nm). The ratio of both contributions varies from one molecule to another. In our case, the distribution of wavelength maxima can be partly explained by the heterogeneities of condensation of the MTEOS precursor after hydrolysis. Despite the limited number of spectra acquired at room temperature, the trend is that we have observed only a few spectra departing from these characteristics. By contrast, different types of LT spectra are observed. Type I has been discussed in the previous section, but two additional types (types II and III) can still be distinguished. They will be successively reviewed in the following.

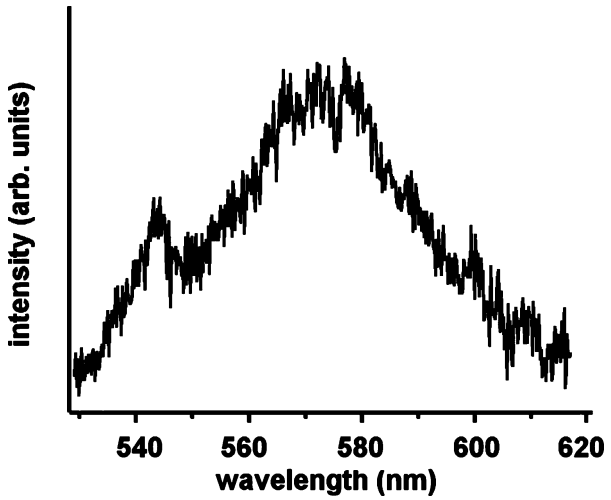

Figure 4. Typical single molecule fluorescence spectrum recorded at room temperature. See text. Same experimental conditions as in Figure 1.

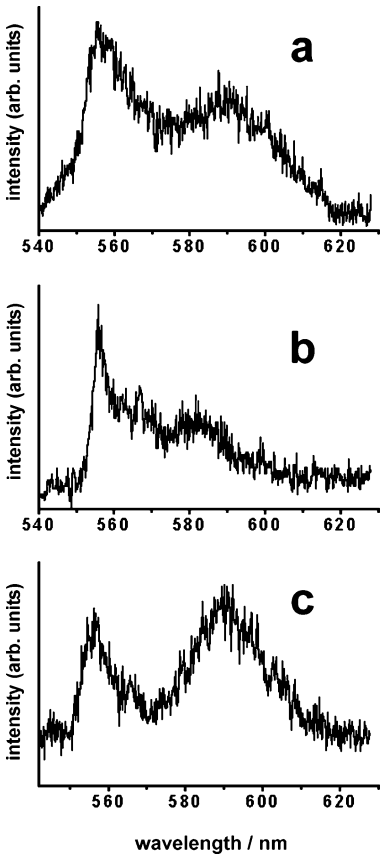

Figure 5. Fluorescence emission of three different molecules exhibiting type II spectra, at low temperature. See text. Same experimental conditions as in Figure 1.

The type II spectrum presents two well-defined lines and sometimes additional vanishing lines. Figure 5 shows typical spectra of type II. It is the most frequently observed type of LT spectrum within those departing from classical fluorescence spectra (≈70%). The well-defined wavelength distribution of the SW line peaks at 557 nm, and it extends on a small wavelength range of about 10 nm. The large number of type II spectra for which the SW line is stronger than or on the same order of intensity as the LW line is at the origin of the relevant peak in the global histogram of the maxima of fluorescence (Figure 2). The center of the LW line distribution is 586 nm, and the wavelengths fall in a range a bit broader, which is illustrated by the histogram of the wavelengths of the two lines of type II LT spectra (Figure 6). The spacing of the two components in each spectrum is nearly constant, on the order of 30 nm. Another characteristic feature is the width of the two lines. The SW line is generally thinner than the LW line and can be structured on its red wavelength wing, whereas the LW line is generally broad and structureless. The features of the type II LT spectra and those of the RT spectra can be described

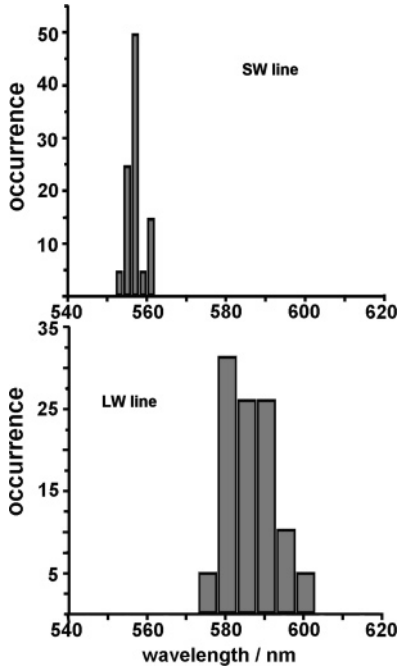

Figure 6. Wavelength distributions of short-wavelength (SW, upper panel) and long-wavelength (LW, lower panel) bands of type II LT single molecule fluorescence spectra.

in the frame of dual fluorescence. Abnormal dual fluorescence, well-known for various organic molecules, derives from the possibility of populating conformers with different twist characters in the excited state. Since the first observation of dual fluorescence in bianthryl[20] and the emphasis put on the importance of electronic reorganization in the excited state, the mechanisms of charge and electron transfer, either in molecules containing well-identified donor and acceptor groups[22−27] or not,[20−21,28−30] have been the object of active studies in relation to the reconformation of the molecule after excitation. Dual fluorescence appears in molecules containing chemical groups able to rotate around a bond that links them to another moiety of the structure. Perylene diimides, together with some other families of molecules, have a large twist of the ground state and no obvious donor or acceptor group. We discuss these characteristics in more detail with respect to dual fluorescence.

Different studies performed on pretwisted phenanthrene compounds[27] or on twisted biphenyls,[23,26] differing, by way of synthesis, by their ground-state twist, have demonstrated that the steric hindrance effect, discussed in relation to type I spectra, is less effective in the excited states than in the ground state. As a result, reorganization toward a more planar conformation is possible in the excited state of a molecule with a largely twisted ground state. The driving force for flattening is a higher mesomeric interaction of the π-electron system. A good example is the case of the 4-*N*,*N*-dimethylamino-2,6-dimethyl-4′-cyanobiphenyl molecule.[23] Two different distributions of rotamers have been predicted to occur in the excited state of this molecule, which already has a 78° twist angle in its equilibrium ground state. One conformer is more planar, while the other conformer is completely twisted with a nearly 90° angle between the two phenyl planes. The dual fluorescence of perylene orange could similarly result from the existence of two rotamers in the excited state, for a given conformation in the ground state.

However, in perylene orange, contrary to the above-mentioned compounds, the two groups in para positions and able to twist around a single bond are identical and do not differ by their electronic character. From this point of view, perylene orange has a behavior close to that of congested benzenehexacarboxylates[30] and has also a similarity to the case of *N*-phenyl-2,3-naphthalimide.[21] It has been noticed in the latter case that the imide biscarbonyl group has a partial acceptor character, resulting from the presence of a partial charge transfer from the N to the O atoms of the carbonyl groups, in the ground state of the molecule. Any relaxation in the excited state of perylene orange toward a more planar conformer leads to an increased interaction between the orbitals of the phenyl groups and those of the perylene core and also favors a possible interaction of the $CH(CH_3)_2$ groups with the core. They can in particular partially overlap the p_z orbitals of the N and O atoms, leading to a partial electronic charge transfer in a more flat emissive state. The analysis can be enlightened by the following experimental observations. We have noticed a relative increase of the weight of the SW emission with respect to the LW one at low temperature, whereas at RT the SW component is very weak or even absent. These results, also observed in the case of benzenehexacarboxylates,[30] have two meanings. First, they indicate that the SW component corresponds to the deexcitation of the less relaxed, more twisted rotamer of perylene orange in its excited state, and second, this rotamer is separated from the fully relaxed, more planar state by an activation barrier at least on the order of the LT thermal energy. We thus propose that, in perylene orange, the LW band of the dual fluorescence results from the deexcitation of the most relaxed state (further named RX), which also corresponds to the more flat rotamer. This conclusion is in line with the results on the *N*-phenyl-2,3-naphthalimide.[21]

The broad width of the LW band and the weakness, if observed, of the SW band at room temperature supports the idea that the potential barrier that separates the two rotamers in the excited state is on the order of or lower than thermal energy at room temperature and that the lifetime of the relaxed Franck−Condon state (further named FC′) is very short. Indeed, a very short relaxation lifetime of the Franck−Condon state is observed in the pretwisted biphenyls, for example. The increase of the SW emission at low temperature indicates that, in this situation, the lifetime of the FC′ state is longer because relaxation to the RX state is partly frozen, in agreement with the fact that the SW emission comes from a conformer with a minor change in twist angle. These results can usefully be compared to the demonstrative results of the room-temperature single molecule study of Meixner et al. on 9-amino-*N*-(2,6-diisopropylphenyl)-perylen-3,4-dicarboximide (API) and *N*,*N*-di-(*tert*-butoxycarbonyl)-API (DAPI) molecules embedded in a polymer matrix.[31] These molecules are also peryleneimides but with clear donor and acceptor groups in para positions. The donor group in the case of DAPI is bulky and cannot rotate to be in plane with the perylene core. The relevant spectrum always displays a structured SW band. By contrast, the donor group of API, NH_2, is less bulky and can rotate under excitation toward a more planar configuration, leading to the observation of a broad structureless LW band. Depending on the location of the API molecule, its spectral dynamics can reveal back-and-forth changes between the two types of spectra. The spectral analysis demonstrates that two conformers exist for API, depending on the twist angle between the amino group and the perylene plane. Moreover, the LW band is also assigned to the most planar conformer and there is a hypsochromic shift to a structured SW emission when the amino group is out of the core plane. Interestingly, in the situation where the LW emission dominates the spectrum, the emission efficiency of these molecules embedded in a polymer is low. In fact, the LW emission in dual fluorescence, which is

favored at room temperature, is often weak. It has been explained in many situations by the activation of new efficient nonradiative decay channels upon reconformation. The weakness of the relevant emission could thus contribute to explain the rather low efficiency of perylene orange that we have observed in sol−gel films. Finally, we observe a slight bathochromic shift for the LW and SW bands upon cooling, for example in the case of bianthryl.[29] As a concluding remark, we can note that the fluorescence spectrum of perylene orange recorded in ethyl acetate is not a mirror image of the absorption spectrum.[11] This has been partly explained by a reabsorption of the emission because of the overlap of the two spectra. A possible alternative explanation, in line with our conclusions, is that the intensity of the second peak is larger than that of the first peak because of dual fluorescence.

In the present sample, the combination of the existence of different conformers for perylene orange with the heterogeneity of the environments of the molecules leads to the observation of several different spectra. We have restricted the paper to the discussion of the most typical and most often observed spectra (namely type I and type II spectra). However, let us briefly mention a last type of spectrum (type III), observed at low temperature. Type III spectra display very weak lines at typical wavelengths, 542 and 550 nm for example, associated with a much stronger but rather broad line generally centered at 580 nm. Different situations can be distinguished with respect to the main line characteristics. First, the line is broad and structureless, and one possibility is that this spectrum corresponds to the LW line of dual emission. As demonstrated by Higgins, ormosil samples show better fluidity compared to tetraalkoxysilane sol−gels because the lower number of Si−O−Si bridges reduces the cross-linking of the silica matrix that is less rigid. As a result, at some sites free of solvents, the molecule can undergo a large geometric reconformation despite low temperature. Second, when the line observed around 580 nm is structured, a possibility is that the line results from the emission of a single conformer, the geometry of which varies in time by jumps. Because of the time acquisition, the line is broadened, but the large width is not related to dual fluorescence. In that case, the molecule can also and alternatively explore very locally a site by translational diffusion. The broadening of the line could reflect a change in the local polarity of the site. Such a situation can be encountered in our ormosil sample, for which residual Si−OH groups as well as CH_3 groups can sit at the pore surface and the molecule can undergo polarity changes, on a nanoscale, by diffusion.

III.3. Spectral Dynamics. To collect additional information, we have recorded successive spectra of different molecules until their photobleaching. Again, various behaviors have been observed in relation to the heterogeneity of the sample. First, let us recall that the probability that two molecules occupy the same pore in our fresh samples is very weak, and that nonpolarized objects have been excluded from analysis. The types of dynamics described below have been observed several times, and they reflect the reorganization of a single molecule under excitation. Some spectra, related to either normal or dual fluorescence, are very stable in time. This is illustrated in Figure 7 for LT spectra. We have also observed intensity fluctuations with or without spectral fluctuations for different types of spectra, as illustrated in Figure 8. These fluctuations could result from so many different effects, such as slow diffusion of the molecule in a chemically or geometrically heterogeneous site, that it would be hazardous to propose a definitive interpretation. It is nonetheless worthwhile to report that often the intensity

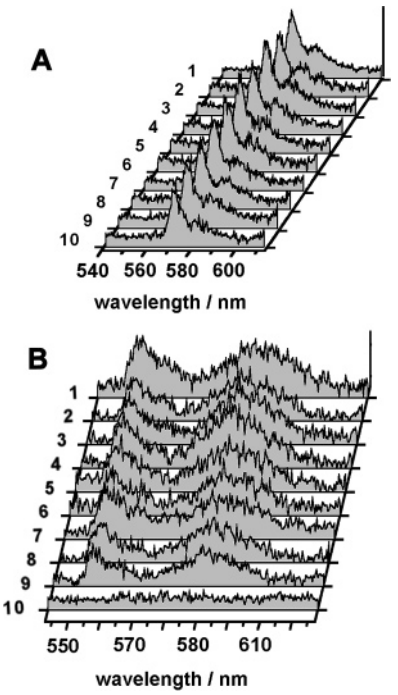

Figure 7. Representative sequences of stable single molecule fluorescence emission: (A) type I spectra; (B) type II spectra, characterized by dual emission. The acquisition time of the successive spectra is 10 s, and the lag time between them is negligible. Successive spectra are numbered on the *z*-axis. Same excitation conditions as in previous figures.

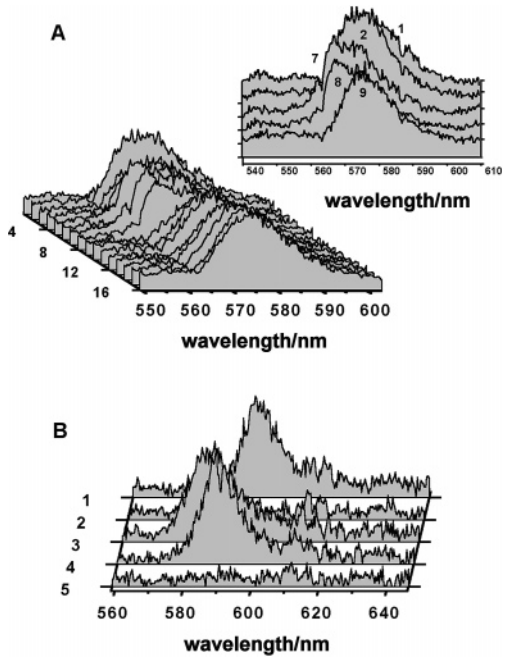

Figure 8. Examples of spectral fluctuations in single molecule fluorescence sequences. (A) Type II room-temperature spectra; characteristic are the spectral jumps. Bottom, the whole sequence; top right, spectra selected to show more clearly the maximum amplitudes of the jumps in the sequence. (B) Type I low-temperature spectra; characteristic is the "long" blinking period (spectrum 2) before the large spectral jump of nearly 13 nm. See Figure 7 for experimental details.

fluctuations as well as the spectral fluctuations are not "continuous". They are frequently followed or interrupted by a period of stability. This is illustrated in Figure 8A in the case of spectral fluctuations observed at room temperature. The maximum displacement in the peak wavelength is 12 nm, but the shifts

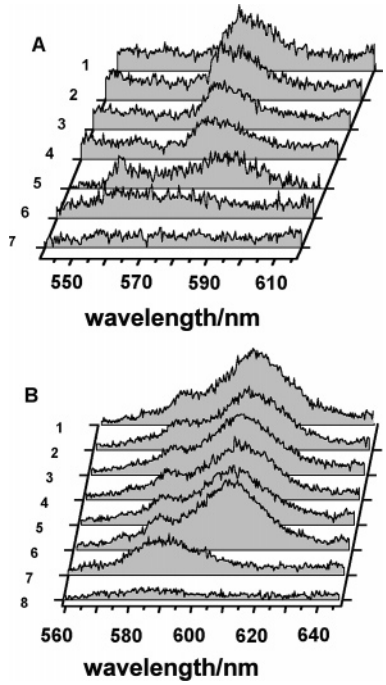

Figure 9. Spectral dynamics representative of transitions between two types of single molecule fluorescence spectra: (A) low-temperature transition from normal fluorescence to dual fluorescence; (B) room-temperature transition between type II fluorescence to normal fluorescence. See text for discussion. See Figure 7 for experimental details.

between successive spectra do not exceed 5 nm. Random shifts are observed during the first nine recordings (90 s), and then the spectrum remains stable during 80 s, after which the molecule bleaches. The spectral shift does not increase monotonically but proceeds by jumps. In the case of molecules doped into a glassy polymer matrix, the latter effect has been interpreted as the result of a slight reorientation of the molecule in time.[32] In our samples, spectral dynamics has also been observed in correlation with blinking as illustrated in the spectrum evolution of Figure 8B, recorded at low temperature. After a first blinking period (spectrum 2, Figure 8B), the fluorescence peak undergoes a blue shift of nearly 13 nm in one step.

Among the various situations we have observed, two can give more insight in the process of dual fluorescence. They are depicted by the dynamics in parts A and B of Figure 9. In case A, obtained at low temperature, the molecule shows a stable normal fluorescence spectrum during four recordings; then at the fifth one, dual fluorescence occurs, it fades, and finally the molecule bleaches. A quick period of blinking was observed at the beginning of the fifth recording. By contrast, in case B (Figure 9B), the RT spectrum of type II is stable for 60 s, and then the LW line, which was the strongest, disappears. At the same time the intensity of the SW line increases, and after 20 s the molecule photobleaches. At the beginning of the seventh recording, we have observed a quick period of blinking on the wide-field imaging. A well-known process for the suppression or decrease of the LW component of a dual emission is hydrogen binding. It can be followed by a quenching of the emission for a period that depends on the time needed for the molecule to retrieve a ground-state conformation with a high probability of excitation. In our sample, there are two reasons for which hydrogen binding can occur. First is the case if the molecule slowly diffuses toward an inner wall with pendant Si−OH. Second, H binding can also occur in the presence of a protic solvent, which could be residual water in our system. Depending on the site, such a process can explain a back-and-forth change between dual and normal fluorescence. Moreover, hydrogen binding can be at the origin of a subsequent change of conformation in the ground state, following the release of hydrogen bonding. These two combined processes could explain the evolutions depicted in Figure 9.

IV. Conclusion

We have studied the spectral behavior of single perylene orange molecules doped into thin sol−gel films. The idea underlying this work was to gain insight into the properties of this dye in sol−gel samples since it had been demonstrated that perylene orange could show an increased photostability. Such samples could thus be good candidates for cheap lasing materials. Our previous results[14,15] on photobleaching indicate, quite surprisingly, that perylene orange is not a very efficient emitter in our ormosil thin films and that, most probably, a dark state of low absorption or low fluorescence yield is involved in the fluorescence cycle. The main results of the present spectral analysis at 173 K are correctly interpreted within the assumption that perylene orange has several conformers in its ground state and possibly two rotamers in the excited state. In particular locations, reconformation can be inhibited or very slow, at this low temperature, in constrained places, and typical spectra (type I) with a thin main line are observed at various discrete wavelengths. Some of the conformers can have either a weak absorption rate or a low fluorescence yield, and they could correspond to the predicted dark states.[15] A reconformation also takes place in the excited states in appropriate locations, leading to the observation of two rotamers. Many molecules showing dual fluorescence type II spectra have an important LW band. At room temperature, the reconformation in the excited states manifests itself by the occurrence of very weak SW peaks and a broad structureless LW band, which corresponds to the most planar rotamer.

Finally, if some conformers have a weak emission yield, the relevant temporal emission trace of the molecule will show a dark or nearly dark period until the molecule undergoes a reconformation, either driven by intramolecular motions of the molecule itself or after translational diffusion to a location with different properties. This type of signature has been frequently observed in temporal traces of single molecules. These dark states could in addition explain why a five electronic level model failed to explain photobleaching results in our samples.

Acknowledgment. We thank Drs J.-P. Boilot and F. Chaput (Laboratoire de la Matière Condensée, UMR 7643 CNRS, Ecole Polytechnique, 91128 Palaiseau Cedex, France) for providing the thin sol−gel films.

References and Notes

(1) Langhals, H. *Chem. Ber.* **1985**, *118*, 4641.

(2) Langhals, H.; Demmig, S.; Huber, H. *Spectrochim. Acta, Part A* **1988**, *44A*, 1189.

(3) Seybold, G.; Wagenblast, G. *Dyes Pigm.* **1989**, *11*, 303.

(4) Löhmannsröben, H.-G.; Langhals, H. *Appl. Phys. B* **1989**, *B48*, 449.

(5) Ivri, J.; Burshtein, Z.; Miron, E.; Reisfeld, R.; Eyal, M. *IEEE J. Quantum Electron.* **1990**, *26*, 1516.

(6) Sadraï, M.; Hadel, L.; Sauers, R. R.; Husain, S.; Krogh-Jespersen, K.; Westbrook, J. D.; Bird, G. R. *J. Phys. Chem.* **1992**, *96*, 7988.

(7) Faloss, M.; Canva, M.; Georges, P.; Brun, A.; Chaput, F.; Boilot, J. P. *Appl. Opt.* **1997**, *36*, 6760.

(8) Rahn, M. D.; King, T. A.; Gorman, A. A.; Hamblett, I. *Appl. Opt.* **1997**, *36*, 5862.

(9) Qian, G.; Yang, Y.; Wang, Z.; Yang, C.; Yang, Z.; Wang, M. *Chem. Phys. Lett.* **2003**, *368*, 555.

(10) Burgdorff, C.; Lohmannsroben, H. G.; Reisfeld, R. *Chem. Phys. Lett.* **1992**, *197*, 358.
(11) Rahn, M. D.; King, T. A. *Appl. Opt.* **1995**, *34*, 8260.
(12) Wang, H.; Bardo, A. M.; Collinson, M. M.; Higgins, D. A. *J. Phys. Chem. B* **1998**, *102*, 7231.
(13) Bardo, A. M.; Collinson, M. M.; Higgins, D. A. *Chem. Mater.* **2001**, *13*, 2713.
(14) Julien, C. Ph.D. Thesis, Université Paris XI, Orsay, France, 2004.
(15) Julien, C.; Débarre, A.; Nutarelli, D.; Richard, A.; Tchénio, P. *J. Phys. Chem. B* **2005**, *109*, 23145.
(16) Higgins, D. A.; Collinson, M. M.; Saroja, G.; Bardo, A. M. *Chem. Mater.* **2002**, *14*, 3734.
(17) Hofkens, J.; Vosch, T.; Maus, M.; Köhn, F.; Cotlet, M.; Weil, T.; Herrmann, A.; Müllen, K.; De Schryver, F. C. *Chem. Phys. Lett.* **2001**, *333*, 255.
(18) Hädicke, E.; Graser, F. *Acta Crystallogr.* **1986**, *C42*, 195.
(19) Klebe, G.; Graser, F.; Hädicke, E.; Berndt, J. *Acta Crystallogr.* **1989**, *B45*, 69.
(20) Schneider, F.; Lippert, E. *Ber. Bunsen-Ges. Phys. Chem.* **1968**, *72*, 1155.
(21) Valat, P.; Wintgens, V.; Kossanyi, J.; Bicszok, L.; Demeter, A.; Berces, T. *J. Am. Chem. Soc.* **1992**, *114*, 946.
(22) Dey, J.; Warner, I. *J. Phys. Chem. A* **1997**, *101*, 4872.
(23) Maus, M.; Rettig, W.; Bonafoux, D.; Lapouyade, R. *J. Phys. Chem. A* **1999**, *103*, 3388.
(24) Rettig, W.; Bliss, B.; Dirnberger, K. *Chem. Phys. Lett.* **1999**, *305*, 8.
(25) Zachariasse, K. A. *Chem. Phys. Lett.* **2000**, *320*, 8.
(26) Maus, M.; Rettig, W. *J. Phys. Chem. A* **2002**, *106*, 2104.
(27) Maus, M.; Rettig, W.; Depaemelaere, S.; Onkelinx, O.; De Schryver, F. C.; Iwai, K. *Chem. Phys. Lett.* **1998**, *292*, 115.
(28) Laguitton-Pasquier, H.; Pansu, R.; Chauvet, J.-P.; Collet, A.; Faure, J.; Lapouyade, R. *Chem. Phys.* **1996**, *212*, 437.
(29) Mac, M.; Kwiatkowski, P.; Pischel, U. *Chem. Phys. Lett.* **2002**, *357*, 440.
(30) Yamasaki, N.; Inoue, Y.; Yokoyama, T.; Tai, A.; Ishida, A.; Takamuku, S. *J. Am. Chem. Soc.* **1991**, *113*, 1933.
(31) Stracke, F.; Blum, C.; Becker, S.; Müllen, K.; Meixner, A. J. *Chem. Phys. Lett.* **2000**, *325*, 196.
(32) Bartko, A. P.; Xu, K.; Dickson, R. M. *Phys. Rev. Lett.* **2002**, *89*, 026101.